Effect of spacing of grid PHD on performance of combined PHD-PVD vacuum preloading method for treatment of clayey slurry

Yu PAN, Ph.D. Postdoc.

College of Civil and Transportation Engineering, Shenzhen University, Shenzhen, China;

email: yu.pan@szu.edu.cn

Ding-Bao SONG, Ph.D., Research Assistant Professor

Department of Civil and Environmental Engineering, The Hong Kong Polytechnic University,

Hung Hom, Kowloon, Hong Kong, China; email: jian-hua.yin@polyu.edu.hk

Zhen-Yu Yin, Ph.D., Professor (Corresponding Author)

Department of Civil and Environmental Engineering, The Hong Kong Polytechnic University,

Hung Hom, Kowloon, Hong Kong, China; email: zhenyu.yin@polyu.edu.hk

Corresponding author, Tel: +852 3400 8470; Fax: +852 2334 6389

Jian-Hua Yin, Ph.D., Chair Professor

Department of Civil and Environmental Engineering, The Hong Kong Polytechnic University,

Hung Hom, Kowloon, Hong Kong, China; email: jian-hua.yin@polyu.edu.hk

Manuscript submitted to *Canadian Geotechnical Journal*

24 November 2023

Abstract:

A novel ground improvement method that combines grid prefabricated horizontal drains (PHDs) with prefabricated vertical drain (PVDs) assisted by vacuum preloading is proposed for the beneficial reuse of dredged clayey slurry for reclamation purpose. To assess the feasibility of this innovative method, physical model tests are designed and conducted using high-water content Hong Kong marine deposits (HKMD) as the clayey slurry material. Furthermore, the impact of the spacing configuration of the grid PHD on the effectiveness of the proposed method is investigated through a series of model tests. A test without the installation of PVD was set, and in this case, two phases of vacuum preloading are applied sequentially through the PHD layer installed in stage. The other three tests involve three phases, with the addition of a vacuum preloading stage through PVD and variations in arrangement pattern of grid PHD layer. Results show that this proposed approach yields a final average undrained shear strength of soil of approximately 30 kPa, meanwhile reducing the average water content to around 50%. Furthermore, it is observed that decreasing the vertical spacing of grid PHDs results in growing final settlement. Reducing the horizontal spacing has less impact on the final settlement.

Keywords: clayey slurry; vacuum Preloading; consolidation; prefabricated horizontal/vertical drain; model test; arrangement pattern

Introduction

Reclamation plays a pivotal role in the development of Hong Kong. However, the scarcity of high-quality granular filling material for such projects presents a substantial challenge. In addition, the local dredged Hong Kong marine deposit (HKMD) extracted from the seabed remains underutilized, posing potential environmental concerns. Consequently, the utilization of locally dredged HKMD as a filling material in reclamation projects emerges as an attractive solution to address both issues. However, HKMD possesses poor engineering attributes, characterized by high water content, low permeability, low strength, and high compressibility (Yin 1999, Feng 2016, Yin and Tong 2011, Koutsoftas et al. 1987). The pressing engineering challenge thus centers on improving the engineering characteristics of HKMD to render it a suitable filling material for reclamation projects.

Prefabricated Vertical Drains (PVDs) assisted by vacuum preloading represents a prominent and well-established method for soft soil improvement, and this method has been proved successful around the world (Kjellman 1952, Yan and Chu 2005, Chu et al. 2000, Tang and Shang 2000, Bergado et al. 2002, Cai et al. 2018, Indraratna et al. 2005, Walker et al. 2009, Walker and Indraratna 2007, Gao and Zhang 2020, Lei et al. 2020). PVDs are installed in the soil to curtail the drainage length, thereby expediting the primary consolidation process. Vacuum preloading reduces atmospheric pressure within the soil, which introduces the gradient in pore water pressure and facilitates the consolidation process. Consequently, the

PVDs vacuum preloading approach stands out as a swift remedy for soft soil treatment. Extensive research on PVDs vacuum preloading includes empirical investigations (Tang and Shang 2000, Bergado et al. 2002, Yan and Chu 2005, Cai et al. 2018) and theoretical studies (Indraratna et al. 2005, Walker et al. 2009, Walker and Indraratna 2007, Gao and Zhang 2020, Lei et al. 2020). Nevertheless, certain limitations may surface when applying this method to dredged soil with high water content. Firstly, the installation of PVDs necessitates a specific soil strength, which is time-consuming when dealing with dredged soil with high water content. Secondly, PVDs may experience bending issues in response to substantial soil settlement, potentially leading to inadequate maintenance of vacuum pressure in the lower soil layers and, consequently, ineffective treatment within these lower regions.

The prefabricated horizontal drains (PHDs) vacuum preloading method emerges as a promising approach for the improvement of dredged soil with high water content, as supported by existing research (Shinsha 1991, Chai et al. 2014, Pu et al. 2022, Song et al. 2022, Shinsha and Kumagai 2014, Menon and Bhasi 2021, Feng et al. 2020). Several merits characterize the PHDs vacuum preloading method's suitability for high-water-content soil treatment: Firstly, PHDs can settle with the soil, thus avoiding the bending issues commonly encountered. Secondly, vacuum preloading can be initiated simultaneously with the filling process since PHDs can be preinstalled at the bottom of the soil, eliminating any strength requirements for the soil. Thirdly, the need for a sealing layer is obviated, as the soil above the PHDs can serve as effective sealing material. The first application of vacuum consolidation method assisted with PHDs in the field test was conducted in Japan (Shinsha

1991). Then, the calculation method of settlement for the vacuum consolidation method assisted with PHDs was proposed based on the plane strain model (Chai et al. 2014). The combination of vacuum consolidation method and flocculation method was studied by model tests (Pu et al. 2022 and Khoteja et al. 2022). The compatibility between geotextile sheets and the PHDs and the effect of geotextile sheets on the vacuum consolidation was studied based on the model tests (Chen et al. 2022). A large-strain calculation model for vacuum consolidation assisted with PHDs was proposed based on the Plan-strain Consolidation settlement model (Fox and Berles 1997, Song et al. 2022 and Song et al. 2023). However, it should be noted that the treatment on the upper soil is not obvious by PHDs vacuum preloading method (Shinsha and Kumagai 2014). Future treatment for the upper soil is required for the PHDs vacuum preloading method. Furtherly, the expeimental studies on PHDs vacuum preloading are still not enough to exhibit the mecahnism of PHDs vacuum preloading, the construction method of PHDs vacuum preloading are still conceptual.

In this paper, a series of physical model tests were conducted using high-water content Hong Kong marine deposits (HKMD) as the clayey slurry material. Furthermore, the impact of the spacing configuration within the grid PHD on the effectiveness of proposed method is investigated through four parallel model tests. In the first test, two phases of PHD vacuum preloading were sequentially applied, with no incorporation of PVD vacuum preloading. In the other three tests, two layers of PHD vacuum preloading and PVD vacuum preloading were employed, with variations in vertical and horizontal grid PHD spacing.

Combined PHD and PVD vacuum preloading method

The vacuum pressure profile within the combined PHD and PVD vacuum preloading method is depicted in Figure 1. For analytical convenience, the vacuum distribution along the depth is typically simplified. It adopts a trapezoidal distribution of PVD vacuum pressure along the depth, as proposed by Indraratna et al. 2005. This trapezoidal distribution effectively captures two key attributes of the actual PVD vacuum pressure distribution: it exhibits its maximum value at the surface and gradually diminishes with depth, while also maintaining a discernible level of vacuum pressure at the bottom. Conversely, a triangular distribution is assumed for PHD vacuum pressure, following the approach outlined by Chai et al. (2014). In this case, the vacuum pressure is assumed to be at its peak at the bottom, and at the surface, it aligns with the characteristics of a free permeable boundary, resulting in zero vacuum pressure along the depth. It shall be specified that this distribution of PHDs vacuum pressure assumes that the surface is unsealed, and it shall be modified for multi-layer soil, which will be discussed in this paper.

Based on the consolidation of the unit cell theory (Biot 1941,Onoue 1988), the effective radius of influence of PVD can be estimated as (Cai et al. 2018)

(1) $$r_e = (15 \sim 22) r_w$$

where r_e is the effective radius of influence of the unit cell; and r_w is the equivalent drain radius of the band drain, which can be calculated by

(2) $$r_w = \frac{a+b}{4}$$

where a and b are the width and thickness of the band drain. According to the equal area principle, the radius of the unit cell in a square layout can be obtained by

$$r = 0.525S \tag{3}$$

where S is the spacing or the PVDs. By setting $r_e = r$, the spacing between adjacent PVDs can be calculated. The application of PHD vacuum preloading in physical model tests or field trials remains rather constrained. Initially, the influence radius of PHD is set to match that of PVDs. Subsequently, a series of physical model tests was undertaken to investigate the impact of spacing of grid PHDs on vacuum consolidation.

Model test design

A specially designed plexiglass model tank, featuring a side length of 30 cm, was employed for the execution of the model tests. As depicted in Figure 2, one side of the tank was equipped with two pore water pressure transducers positioned at a vertical interval of 100 mm. There were four sampling ports in the middle of each section on the opposite side. A measuring tape was affixed to the front of the model tank to facilitate the measurement of soil and water heights. A camera was positioned to capture the test proceedings and monitor soil settlement development throughout. Additionally, a settling column was placed nearby to provide a basis for comparing PHD vacuum preloading with self-weight consolidation. The vacuum system is comprised of essential components including a vacuum pump, a suction filter barrel, multiple vacuum gauges, drainage pipes, and an electronic scale designed to measure the weight of discharged water.

Material

Soil properties

The soil of the four model tests was taken from Tuen Mun, Hong Kong with brownish-grey color. Its natural water content ranged from 80% to 90%, the initial water content used in the three model tests is 200%. The properties of the HKMD are listed in Table 1. The particle size distribution curve is shown in Figure 3, and the detailed content of each mineral is listed in Table 1.

The reconstituted soil sample with an initial water content of 200% was used to conduct the multi-stage loading oedometer tests. It shall be noted that a pulley system is used to balance the initial weight above the soil specimen, ensuring the pressure above the soil specimen is 0 kPa during the preparation process. The pressure is then applied by the pulley system, which can be set as low as 0.1 kPa (Song et al. 2024). The relationship between vertical effective stress and void ratio is shown in Figure 4, the initial compression index (C_c) of 0.796, rebound index (C_r) of 0.194, and secondary consolidation index ($C_{\alpha e}$) of 0.0224 were determined from the multi-stage loading oedometer tests.

Triaxial tests

Triaxial tests were conducted to investigate the stress-strain relationship of the HKMD used in the model tests. Two stress-line consolidated, undrained triaxial compression tests were conducted on HKMD 1 soil under overconsolidation ratios (OCR) of 1 and 4, considering the potential impact of vacuum preloading on the stress history of the soil. The

142 GDS triaxial apparatus are used to provide a relatively rigid axial loading system to
143 investigate the strain-rate effects and relaxation features of th0.e stress-line consolidated soils.
144 The stress-line consolidation was conducted by increasing the cell pressure and external load,
145 the external load was increased with a relatively low rate to avoid causing too much lateral
146 deformation. After the consolidation, the undrained shearing test was conducted. During the
147 undrained shearing test, the cell pressure was maintained at a constant value. The strain rate
148 for the two tests was applied at a sequence as: +2%/hr. +0.2%/hr, +20%/hr, -2%/hr
149 (unloading), and +2%/hr (reloading). The test results are shown in Figure 5, the calculated
150 friction angle of the soil is 31°. The peak shear stress of the soil is observed to be 105 kPa and
151 126 kPa under OCR values of 1 and 4, respectively, highlighting the effect of
152 overconsolidation on enhancing soil strength. Additionally, the strain rate-dependent behavior
153 of this soil sample is evident and should be considered in the future design of construction
154 work above it.

155 **Properties of prefabricated band drain**

156 The prefabricated band drains used in the model test is a new type of anti-clogging
157 drains as reported by Cai et al. 2017. The filter is affixed to the core, rendering each core an
158 individual drainage pathway. This configuration augments the stiffness of board drains and
159 mitigates the clogging issues within the drains. The parameters of the prefabricated band
160 drains are listed in Table 2.

Test scheme

The duration of applying vacuum preloading and filling the initial slurry is illustrated in Figure 6 and Figure 7. A summary of the features of each model test is listed in Table 3 and the sketch of each model test is shown in Figure 8. The spacing of PVDs ranges from 0.5 m to 2 m in practice, with the typical width of a band drain being 100 mm. Consequently, the ratio of PVD spacing to band drain width ranges from 5 to 20, which is a key parameter in the design of PVDs and the calculation of the area replacement ratio. In our model tests, the side length of the box is 300 mm, and the width of the band drains is trimmed to 30 mm or 60 mm, as listed in Table 3. Therefore, the ratio of PVD spacing to band drain width in our model tests is 5 and 10, within the practical ratio range.

The grid shape of the first model test is different from the other three model tests, which aims to investigate the boundary effect on the vacuum consolidation. In the meanwhile, a settling column test was conducted to compare the settlement rate of self-weight consolidation and PHDs vacuum preloading. The detailed test steps of each model tests are illustrated in the following:

The testing steps for the first model test unfolded as follows:

Step 1: The initial phase involved the installation of the bottom layer grid PHDs, vacuum gauges at various positions, along with a tape measure. Subsequently, soil was filled into the tank to a height of 700 mm.

Step 2: The staged vacuum preloading was initiated. Vacuum levels ranged from 20 kPa to 80 kPa, with increments of 20 kPa. Each stage persisted for one day, after which the vacuum pressure was maintained at 80 kPa. This stagged loading method is used to avoid fast accumulation of fine particles in the adjacent of board drains, which occurred in previous pretests when vacuum pressure was initially set to be 80 kPa, accompanied with quick decrease in drainage efficiency. The maximum vacuum pressure can reach up to 100 kPa; however, some loss of vacuum pressure along the conduction pathway is unavoidable. According to Chu et al. 2008, the vacuum pressure is typically maintained at 80 kPa in practice. Therefore, an 80 kPa vacuum pressure is used to simulate practical conditions.

During this stage, monitoring encompassed settlement, vacuum pressures, pore water pressure, and the weight of discharged water. Additionally, water content and undrained shear strength were measured upon completion.

Step 3: The second layer of PHD along with vacuum gauges was installed. Soil was then filled into the tank, covering the bottom layer of soil, to a height of 700 mm.

Step 4: Upon concluding the model test, undrained shear strength and water content tests were implemented along the depth to provide the profiles of water content and undrained shear strength.

The detailed design of the transducers of the second model test is shown in Figure 9. The test regimen for the second model test was similar to the first three steps of the initial model test, but the initial thickness of each soil layer was 500 mm. Moreover, PVDs and

vacuum gauges were introduced after the PHDs vacuum preloading process. Vacuum preloading was then activated on the PVDs. Finally, Step 4 of the first model test was replicated in the second model test.

The third model test closely paralleled the second model test, with the primary distinction being the initial height of each soil layer, set at 700 mm. The installation of transducers in the third model test closely resembled the setup in the second model test. Lastly, the fourth model test duplicated the steps of the second model test, with the sole difference being a boarder band width of the board drains, added to 60 mm.

Test results

The settlement, the discharged water, excess pore water pressure, water content, and undrained shear strength were measured to evaluate the efficiency of the proposed method and study the mechanism of the PHDs vacuum preloading.

Discharged water

The drainage efficiency of both PHD vacuum preloading and PVD vacuum preloading is assessed by tracking the weight of drained water. In this evaluation, a measure termed the thickness of discharged water is introduced, it is calculated as the drained volume divided by the surface area of the model tank.

The installation of PHD grids differs between the first and third model tests, despite having the same area of PHD grids. In the first model test, the PHD grids are placed along the

central cross line, while in the third model test, they are placed at the edge. However, the trends observed in Figure 10a for the first and third model tests during the PHDs vacuum preloading stage are similar, indicating that boundary effects may be disregarded in this scenario. The discharging rate results, illustrated in Figure 10b, indicate maximum discharging rates of 7.1 cm/day, 3.7 cm/day, 7.2 cm/day, and 3.6 cm/day for the four model tests. Notably, the highest discharging rate occurs at the onset of vacuum preloading and subsequently diminishes over time. This phenomenon is attributed to the decrease in the soil permeability, leading to a reduction in the transfer of vacuum pressure from the drains to the soil and a corresponding decline in the rate of water drainage, in accordance with Darcy's law.

Settlement

The total settlement development across all four model tests is depicted in Figure 10*b*. In the context of the first model test, the total settlement reaches 32.4 cm upon completing vacuum preloading on the bottom layer PHD, which is approximately 4.8 times greater than the settlement observed in the settling column test. This demonstrates the improved efficiency of PHD vacuum preloading. Two points can be observed from the result: Firstly, the settlement rate experiences an initial surge upon the application of vacuum preloading, followed by a gradual reduction over time. This phenomenon can be attributed to the initial generation of substantial negative pore water pressure during vacuum preloading, resulting in increased seepage rates. As time progresses, fine-grained particles accumulate around the PHD, forming a dense layer that curtails the transfer of vacuum pressure from the PHD and reduces the permeability of the surrounding soil. Secondly, upon introducing the second layer

of soil and applying vacuum pressure, the settlement rate of the bottom soil layer increases due to the additional load imposed by the second layer. Notably, the settlement rate of the second soil layer outpaces that of the bottom layer. Specifically, the second layer exhibits a 30.9 cm settlement within 40 days, whereas the bottom layer records a 39.1 cm settlement over a span of 72 days. This discrepancy arises because both the top and bottom surfaces of the second soil layer serve as permeable boundaries, whereas only the top surface of the first soil layer is permeable. Consequently, the drainage path length for the second soil layer is only half that of the bottom soil layer.

Pore water pressure

As depicted in Figure 11*a*, the transfer of vacuum pressure from the PHD to the surrounding soil is contingent upon the distance between the soil and the PHD, necessitating a waiting period. Notably, the influence of vacuum preloading is intricately linked to the proximity of the soil to the PHD. For instance, PPT 1, positioned closest to the PHD (a mere 10 cm above the bottom PHD), registers the most substantial pore water pressure. Over time, its pore water pressure ultimately reaches a magnitude of -70 kPa. In contrast, PPT 2 was placed at a distance of 20 cm above the bottom PHD, where the maximum pore pressure observed was -30 kPa, considerably smaller compared to PPT 1. PPT 3 recorded an even larger excess pore water pressure than PPT 2. This difference is due to PPT 3 being positioned close to the second layer of PHD at the end of the first model test.

In the second model test, illustrated in Figure 11*b*, an obvious increase in pore pressure is noted following the application of PVD vacuum preloading. The maximum pore water pressure reaches -80 kPa during the staged vacuum preloading of the PVD. Conversely, in the third model test as shown in Figure 11*c*, the maximum pore water pressure recorded is -65 kPa. The increase of 20 cm in the soil layer thickness leads to a decrease of -17 kPa in pore water pressure. This suggests adopting a thickness of 50 cm to ensure the effectiveness of vacuum preloading treatment. In the fourth model test, as depicted in Figure 11*d*, the overall trend is similar to that of the second model test. Notably, variations in the width of the band drains have minimal influence on the pore water pressure.

Consolidation properties after treatment

Multi-stage oedometer tests were conducted on soil samples following vacuum treatment, which reduced the water content to 50%. The tests determined a compression index (C_c) of 0.189, a rebound index (C_r) of 0.026, and a secondary consolidation index ($C_{\alpha e}$) of 0.0034. These results indicate that the compressibility of the soil has been significantly improved by the vacuum treatment.

Water content and undrained shear strength

The vane shear tests were conducted in three horizontal positions (near the PHD, in the middle of PHD and PVD, near PVD) at different depths and soil samples at these locations were collected for water content tests. The test results of four model tests are shown in Figure 12.

279 The undrained shear strength profile of the first model test is shown in Figure 12*a*. The
280 undrained shear strength is largest near the bottom, reaching 26.5 kPa. While the change in
281 undrained shear strength is not significant in the soil between the second layer PHD and the
282 bottom layer PHD, it decreases noticeably above the second layer PHD. Comparing the
283 results at different horizontal positions, it can be concluded that the closer the horizontal
284 distance to the PHD, the greater the shear strength obtained. However, it should be noted that
285 the shear strength of the upper soil did not increase sufficiently to support future machinery
286 work. As shown in Figure 12*b*, the water content at the bottom is the lowest, with a value of
287 55%. It ranges from 55% to 61% between the two layers of PHD and increases from 58% to
288 99% from the second layer PHD to the top soil surface. There is a notable correlation
289 between the water content of the soil and the undrained shear strength. When the initial water
290 content is higher than 70%, the undrained shear strength remains close to 0 kPa. However, as
291 the water content decreases from 70% to around 52% (the liquid limit), the undrained shear
292 strength increases significantly.

293 As shown in Figure 12*d* and Figure 12*e*, the trend observed in the second model test
294 differs from that of the first model test. Although an inflection point can still be found around
295 the height of the second layer of PHD, the treated soil in the second model test appears more
296 uniform and exhibits higher undrained shear strength, with a maximum value of 38 kPa. The
297 results of the second model test indicate that the combined treatment of PHD vacuum
298 preloading and PVD vacuum preloading effectively improves the super-soft soil in two key
299 aspects: Firstly, the water content can be decreased to an average level below the liquid limit,

300 resulting in higher undrained shear strength compared to PHD vacuum preloading alone.
301 Secondly, the soil is significantly more uniform than that treated by PHD vacuum preloading
302 only, particularly with much higher strength observed in the upper soil layers. It should be
303 noted that the undrained shear strength in the third model test is smaller than that in the
304 second and fourth model tests. This is because the larger vertical spacing introduces a longer
305 drainage path, resulting in lower treatment efficiency.

306 **Vacuum pressure distribution**

307 To obtain the vacuum pressure distribution of the grid PHDs, four vacuum gauges are
308 placed at different heights of the soil, their initial height are shown as Figure 9.

309 The development of vacuum pressure in soil with time is shown in Figure 13. It can be
310 deduced that vacuum pressure takes time to be transferred from the board drains to the soil
311 nearby, which can also be found in other physical model tests (Chen et al. 2022). A key point
312 is that the treating effect of the soil is largely influenced by the maximum vacuum pressure,
313 so that the focus is the maximum vacuum pressure at the end of each construction stage. The
314 vacuum pressure applied in the PVD and PHDs are set to be 80 kPa. The vacuum pressure at
315 Point A reaches to -23 kPa at the end of the first layer soil treatment, and it reaches to -40 kPa
316 at the end of the second layer soil treatment, its value increased to -75 kPa after the PVD
317 vacuum preloading is applied. The development of vacuum pressure in Point A shows the
318 combined effect of PHD and PVD vacuum preloading. The vacuum pressure grows to around
319 55% of the applied vacuum pressure during the PHD vacuum preloading stage, this indicates

320 that the vacuum pressure will also decrease in horizontal plane when it is away from the
321 PHDs. The vacuum pressure grows to around 94% of the applied vacuum pressure during the
322 PVD vacuum preloading stage, which means that the soil is furtherly strengthened by the
323 PVD vacuum preloading, thus a better treatment of the combined method can be achieved.

324 A simplified linear empirical suction line of PHDs vacuum preloading is proposed based
325 on the monitoring data of vacuum pressure:

326 (4)
$$u_s(z)=\begin{cases} s*\dfrac{z}{z_2}\left(z\in(z_2,0)\right. \\ s*\left|\dfrac{2z-(z_1+z_2)}{(z_2-z_1)}\right|+\dfrac{s}{2}\left(z\in(z_1,z_2)\right. \end{cases}$$

327 where s is the vacuum pressure applied, z_2 and z_1 are the depth of the second layer and the
328 first layer of soil, z is the depth of the soil. The proposed suction line aims to capture three
329 important features of the PHD vacuum pressure distribution: the vacuum pressure is 0 near
330 the surface; the vacuum pressure near the PHDs is largest; the vacuum pressure will decrease
331 with the increase of the distance to the PHDs.

332 The comparisons of proposed suction line and the measured data at the end of the PHDs
333 vacuum preloading are shown in Figure 14. A reduction index of 0.5 is considered as the
334 measured point is at the middle position of the grid PHDs. The regression analysis yielded R^2
335 values of 0.93 and 0.88 for the vacuum pressure distribution of one-layer PHDs and two-layer
336 PHDs, respectively. These results indicate a strong correlation between the proposed suction
337 line and the measured data, demonstrating a high degree of fit. It shall be specified that the
338 variations of vacuum pressure at different locations is unignorable because of the nonlinear

soil properties during the vacuum preloading stage, which furtherly introduces much uncertainty to the vacuum pressure distribution. More monitored data is expected to reveal the real vacuum pressure distribution. It should be noted that this proposed suction line is applicable only to the boundary conditions present in this model test, where the surface is permeable and the bottom is impermeable during the PHDs assisted with the vacuum preloading stage. Further tests are necessary to predict the vacuum pressure distribution under different boundary conditions.

Consolidation degree

The degree of consolidation is usually used to assess the effectiveness of the ground improvement method like the surcharging preloading and the vacuum preloading. There are two kinds of different methods to calculate the degree of consolidation, the first method is proposed by Asaoka 1978 using the observed settlement data, another method is proposed by Chu and Yan 2005 using the monitored pore water pressure data. The DOC are calculated by two methods to assess the degree of consolidation at the end of each construction stages.

The Asaoka's graphical settlement prediction method using a series of settlement data (S_1, S_2, …, S_{i-1}, S_i, S_{i+1},…, S_N) at constant time intervals, and they are plotted in a S_i versus S_{i-1} plot (i=1,…, N) as shown in Figure 15, the intersecting point of the line with the 45° is regarded as the ultimate settlement S_{ult}. The average DOC of four physical model tests at the end of different construction stages are calculated and the results are listed in Table 4. The Stage 1, Stage 2, and Stage 3 represents the first layer PHD vacuum preloading, the second

359 layer PHD vacuum preloading, and the PVD vacuum preloading respectively. It shall be note
360 that the results may be largely influenced by the time interval selected in the calculation
361 procedure.

362 Another method proposed is proposed by Chu and Yan 2005, the average degree of DOC can
363 be calculated based on the measured pore water pressure at different height. It can be
364 calculated as follows:

365 (5) $$U_{avg}=1-\frac{\int[u_t(z)-u_s(z)]dz}{\int[u_0(z)-u_s(z)]dz}$$

366 where $u_t(z)$ is the final pore water pressure at depth z; $u_s(z)$ is the suction at depth z; $u_0(z)$ is
367 the initial pore water pressure at depth z. The integral in the numerator and denominator in Eq.
368 (4) are the area between the curve of $u_t(z)$ and $u_s(z)$, the integral in the denominator in Eq. (4)
369 are the area between the curve of $u_0(z)$ and $u_s(z)$. The typical calculation of DOC of the
370 second model test are shown in Figure 16. Thus, the average consolidation degree calculated
371 by two methods is listed in Table 4. It can be noticed that the average consolidation degree
372 calculated by the pore water pressure is much smaller than that of the settlement data, this
373 phenomenon was also reported by Chu and Yan 2005. There are several reasons: the shorter
374 calculation steps tend to obtain a smaller ultimate settlement, which will overestimate the
375 consolidation degree; the pore water pressure transducers were installed at limited locations
376 and their depths changes during the consolidation process, which leads to an underestimated
377 measured value of pore water pressure, thus the average consolidation degree is
378 underestimated by the pore water pressure data. However, the average consolidation degree

calculated by both methods are important for the real cases, there are limitations existed on both methods, like the uncertainties of the ultimate settlement of the settlement prediction method, the space variations on the pore water pressure of the pore water pressure method. These two methods can provide a reference range of the average consolidation degree.

Parametric study of grid PHDs spacing

The effects of PHDs spacing on vacuum consolidation are studied through the analysis of the model tests results, and furtherly to reveal the influence zone of PHDs vacuum preloading method. There are three design parameters for the PHDs spacing, the band width w, vertical spacing S_v, and horizontal spacing S_h. The ratio of S_v versus S_h is denoted as SR. The ratio of the area of PHDs versus the area of treated soil are defined as m, which also may be defined as the area displacement ratio. The two ratios are studied to feature the effect of PHDs spacing on vacuum preloading.

Effect of vertical spacing of grid PHDs

The investigation into the vertical spacing of grid PHDs involved a comparative analysis of the second and third model tests. These tests primarily differed in the thickness of the soil layer, which corresponded to the initial vertical spacing of the grid PHDs. The spacing ratio (SR) for the second and third model tests was 1.67 and 2.33, respectively.

The vertical strain behavior across various loading stages is depicted in Figure 17*a*. In general, it is observed that the vertical strain in the model test with an SR value of 2.33 is less pronounced than in the test with an SR value of 1.67. However, an interesting contrast is

399 noted at the conclusion of the first layer of PHDs vacuum preloading. This discrepancy arises
400 primarily due to the shorter treatment duration of the first layer of PHDs vacuum preloading
401 in the second model test compared to the third model test. Figure 17*b* and Figure 17*c* present
402 the average water content and undrained shear strength at the conclusion of different loading
403 stages. These two parameters exhibit a clear interdependence. Smaller SR values correspond
404 to lower water content and higher undrained shear strength. Generally, the second model test
405 demonstrates more uniform and superior treatment effects, consequently affirming the
406 recommendation for a vertical spacing of 500 mm for grid PHDs.

407 **Effect of horizontal spacing of grid PHDs**

408 The analysis of horizontal spacing in the grid PHDs involves a comparative examination
409 of the second and fourth model tests. These tests solely vary in the width of the drainage
410 bands. The parameter *m* for the second and fourth model tests is 0.19 and 0.36, respectively.

411 Vertical strain patterns across various loading stages are illustrated in Figure 17*d*.
412 Notably, vertical strain is significantly greater with a larger *m* value, particularly at the
413 conclusion of the first layer of PHDs vacuum preloading. However, it converges to nearly
414 identical values at the conclusion of the second layer of PHDs vacuum preloading and PVD
415 vacuum preloading. Figure 17*e* and Figure 17*f* exhibit the average water content and
416 undrained shear strength at the conclusion of different loading stages. It becomes evident that
417 the water content and undrained shear strength between the two model tests primarily differ
418 at the conclusion of the first layer of PHD vacuum preloading. In contrast, they closely align
419 at the conclusion of the second layer of PHD vacuum preloading and PVD vacuum

preloading. Consequently, it can be inferred that increasing the *m* value from 0.19 to 0.26 exerts minimal influence on the final soil treatment effectiveness.

Conclusions

This study introduces a novel ground improvement approach, which combines grid PHDs and PVD assisted by vacuum preloading, as a potential solution for land reclamation projects dealing with high water content Hong Kong marine deposits (HKMD). To comprehensively evaluate this method and explore its optimization, a series of four model tests were conducted. These tests served a dual purpose: comparing the proposed combined method with conventional PHD vacuum preloading and investigating the impact of varying vertical and horizontal grid PHD spacings. The outcomes of these model tests unequivocally affirm the effectiveness of the grid PHD and PVD vacuum preloading combined method for rapidly treating highly compressible soil. Key insights derived from the results of three model tests are as follows:

Firstly, when subjected to PHD and PVD vacuum preloading, soil water content can be substantially reduced to approximate the liquid limit, accompanied by a significant increase in undrained shear strength compared to treatment with PHD vacuum preloading alone. Notably, the combined treatment results in a more uniform soil condition, with a marked improvement in the upper soil layers.

Secondly, an empirical suction line of PHDs vacuum preloading is proposed based on the monitoring data of vacuum pressure at different heights, which describes three important

features of the PHDs vacuum pressure distribution: the vacuum pressure is 0 near the surface; the vacuum pressure near the PHDs is largest; the vacuum pressure will decrease with the increase of the distance to the PHDs. The comparisons between the proposed suction line and the measured proves good consistency.

Thirdly, the efficacy of soil treatment is notably contingent on the proximity of PHDs. As the distance to the PHDs decreases, shear strength increases, while water content decreases. This phenomenon arises from the attenuation of vacuum pressure by the dense soil layer surrounding the PHDs. Conversely, greater distances from the PHDs correspond to reduced vacuum pressure and diminished treatment effectiveness. This innovative approach holds promise for future reclamation projects.

Lastly, a vertical spacing of 500 mm for the grid PHD is recommended based on the test results, as it yields superior treatment effects compared to a 700 mm spacing. Interestingly, increasing the area replacement ratio from 0.19 to 0.36 did not yield significant improvements in soil quality. It's essential to note that these tests represent a preliminary investigation into optimal grid PHD spacing, and further research in this area is warranted.

Acknowledgments:

The work in this paper is supported by a Research Impact Fund (RIF) project (R5037-18), a Theme-based Research Scheme Fund (TRS) project (T22-502/18-R), and three General Research Fund (GRF) projects (PolyU 152179/18E; PolyU 152130/19E; PolyU 152100/20E) from Research Grants Council (RGC) of Hong Kong Special Administrative Region

460 Government of China. The authors also acknowledge the financial supports from Research
461 Institute for Sustainable Urban Development of The Hong Kong Polytechnic University and a
462 grant ZDBS from The Hong Kong Polytechnic University.
463
464

465 **References**

466 Yin J-H (1999) Properties and behaviour of Hong Kong marine deposits with different clay
467 contents. Canadian Geotechnical Journal 36 (6):1085-1095.

468 Feng W (2016) Experimental study and constitutive modelling of the time-dependent stress-
469 strain behavior of soils.

470 Yin J-H, Tong F (2011) Constitutive modeling of time-dependent stress–strain behaviour of
471 saturated soils exhibiting both creep and swelling. Canadian Geotechnical Journal 48
472 (12):1870-1885.

473 Koutsoftas DC, Foott R, Handfelt LD (1987) Geotechnical investigations offshore Hong
474 Kong. Journal of Geotechnical Engineering 113 (2):87-105.

475 Kjellman W Consolidation of clay soil by means of atmospheric pressure. In: Proc. Conf. on
476 Soil Stabilization, MIT, 1952. pp 258-263.

477 Yan S-W, Chu J (2005) Soil improvement for a storage yard using the combined vacuum and
478 fill preloading method. Canadian Geotechnical Journal 42 (4):1094-1104.

479 Chu J, Yan S, Yang H (2000) Soil improvement by the vacuum preloading method for an oil
480 storage station. Geotechnique 50 (6):625-632.

481 Tang M, Shang J (2000) Vacuum preloading consolidation of Yaoqiang Airport runway.
482 Geotechnique 50 (6):613-623.

Bergado DT, Balasubramaniam A, Fannin RJ, Holtz RD (2002) Prefabricated vertical drains (PVDs) in soft Bangkok clay: a case study of the new Bangkok International Airport project. Canadian Geotechnical Journal 39 (2):304-315.

Cai Y, Xie Z, Wang J, Wang P, Geng X (2018) New approach of vacuum preloading with booster prefabricated vertical drains (PVDs) to improve deep marine clay strata. Canadian Geotechnical Journal 55 (10):1359-1371.

Indraratna B, Rujikiatkamjorn C, Sathananthan I (2005) Analytical and numerical solutions for a single vertical drain including the effects of vacuum preloading. Canadian Geotechnical Journal 42 (4):994-1014.

Walker R, Indraratna B, Sivakugan N (2009) Vertical and radial consolidation analysis of multilayered soil using the spectral method. Journal of geotechnical and geoenvironmental engineering 135 (5):657-663.

Walker R, Indraratna B (2007) Vertical drain consolidation with overlapping smear zones. Geotechnique 57 (5):463-467.

Gao Y-B, Zhang Z (2020) Vertical compression of soft clay within PVD-improved zone under vacuum loading: Theoretical and practical study. Geotextiles and Geomembranes 48 (3):306-314.

Lei H, Feng S, Edgard CC, Zhou J, Jiang M (2020) Numerical analysis on ground improvement of vacuum preloading with prefabricated radiant drain. Japanese Geotechnical Society Special Publication 8 (13):514-519.

Shinsha H (1991) Improvement of very soft ground by vacuum consolidation using horizontal drains. GEO-COAST, Yokohama, 1991:3-6.

Chai J, Horpibulsuk S, Shen S, Carter JP (2014) Consolidation analysis of clayey deposits under vacuum pressure with horizontal drains. Geotextiles and Geomembranes 42 (5):437-444.

508 Pu H, Khoteja D, Zhou Y, Pan Y (2022) Dewatering of dredged slurry by horizontal drain
509 assisted with vacuum and flocculation. Geosynthetics International:1-13.

510 Song D, Pu H, Khoteja D, Li Z, Yang P (2022) One-dimensional large-strain model for soft
511 soil consolidation induced by vacuum-assisted prefabricated horizontal drain. European
512 Journal of Environmental and Civil Engineering 26 (11):5496-5516.

513 Shinsha H, Kumagai T (2014) Bulk compression of dredged soils by vacuum consolidation
514 method using horizontal drains. Geotechnical Engineering 45 (3):78-85.

515 Menon AR, Bhasi A (2021) Numerical investigation of consolidation induced by
516 prefabricated horizontal drains (PHD) in clayey deposits. Geotechnical and Geological
517 Engineering 39 (3):2101-2114.

518 Feng J, Ni P, Chen Z, Mei G, Xu M (2020) Positioning design of horizontal drain in
519 sandwiched clay-drain systems for land reclamation. Computers and Geotechnics
520 127:103777.

521 Khoteja D, Zhou Y, Pu H, Pan Y (2022) Rapid treatment of high-water-content dredged
522 slurry using composite flocculant and PHD-facilitated vacuum. Marine Georesources &
523 Geotechnology 40 (3):297-307.

524 Chen H, Chu J, Guo W, Wu S (2022) Land reclamation using the horizontal drainage
525 enhanced geotextile sheet method. Geotextiles and Geomembranes.

526 Wu J, Ouyang C, Dai M, Gao Z, Fu H, Wang J (2022) Effect of surcharge loading rate on the
527 performance of surcharge–vacuum preloading with prefabricated horizontal drains.
528 Marine Georesources & Geotechnology:1-9.

529 Song DB, Pu HF, Yin ZY, Min M, Qiu JW (2023) Plane‐strain model for large strain
530 consolidation induced by vacuum‐assisted prefabricated horizontal drains. International
531 Journal for Numerical and Analytical Methods in Geomechanics.

532 Seah TH (2006) Design and construction of ground improvement works at Suvarnabhumi
533 Airport. Geotechnical Engineering 37 (3):171.

534 Yan H, Cao D (2005) Application of low-level vacuum preloading technique in offshore
535 projects. Ocean and River Hydraulics 3:41-43.

536 Biot MA (1941) General theory of three - dimensional consolidation. Journal of applied
537 physics 12 (2):155-164.

538 Onoue A (1988) Consolidation by vertical drains taking well resistance and smear into
539 consideration. Soils and Foundations 28 (4):165-174.

540 Asaoka A (1978) Observational procedure of settlement prediction. Soils and foundations 18
541 (4):87-101.

542 Chu J, Yan S (2005) Estimation of degree of consolidation for vacuum preloading projects.
543 International Journal of Geomechanics 5 (2):158-165.

544

List of table captions

Table 1 Basic soil properties of the HKMD used in the model tests

Property	HKMD
Liquid limit (%)	52.17
Plastic limit (%)	27.17
Plasticity index (%)	25
Particle density (g/cm^3)	2.62
Fine gravel content (%)	3.23
Sand content (%)	14.46
Silt content (%)	63.69
Clay content (%)	18.62

Table 2 Characteristics of prefabricated band drains

	Performance index	Value
Integrated body	Thickness (mm)	4
	Width (mm)	100
	Tensile strength (kN/10 cm)	≥2.4
	Discharge capacity (cm^3/s)	≥50
	Bending resistance (times)	5
Filter	Tensile strength (N/cm)	≥20
	Permeability coefficient (cm/s)	5.0×10^{-3}
	Apparent opening size (um)	120

Table 3 Summary of four model tests

	First model test	Second model test	Third model test	Fourth model test
Band width	30 mm	30 mm	30 mm	60 mm
PVD vacuum preloading	NO	Yes	Yes	Yes
Vertical spacing	700 mm	500 mm	700 mm	500 mm
Area replacement ratio	0.19	0.19	0.19	0.36

Table 4 Summary of DOC of four model tests using two calculation methods

Average DOC	Based on settlement data			Based on pore water pressure data		
	Stage 1	Stage 2	Stage 3	Stage 1	Stage 2	Stage 3
First model test	80%	93%	-	69%	80%	-
Second model test	84%	93%	96%	73%	80%	83%
Third model test	80%	92%	95%	69%	79%	82%
Fourth model test	85%	93%	96%	71%	82%	84%

List of figure captions

Figure 16–Pore water pressure distribution profile of the second model test: (a) after one layer PHDs vacuum preloading; (b) after two layer PHDs vacuum preloading; (c) after two layer PHDs vacuum preloading and PVD vacuum preloading

Figure 17–Parametric studies: (a) vertical strain of different SR; (b) water content of different SR; (c) undrained shear strength of different SR; (d) vertical strain of different *m*; (e) water content of different *m*; (f) undrained shear strength of different *m*

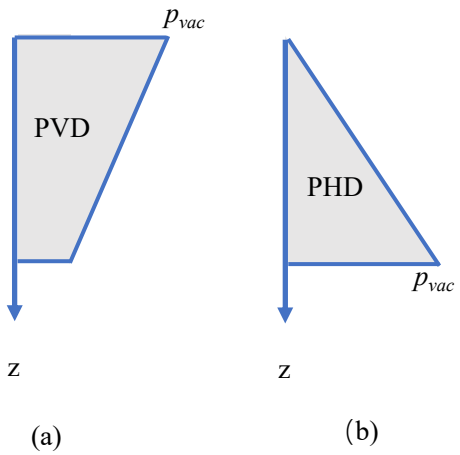

Figure 1–Vacuum pressure distribution along the depth: (a) PVD vacuum preloading; (b) PHD vacuum preloading

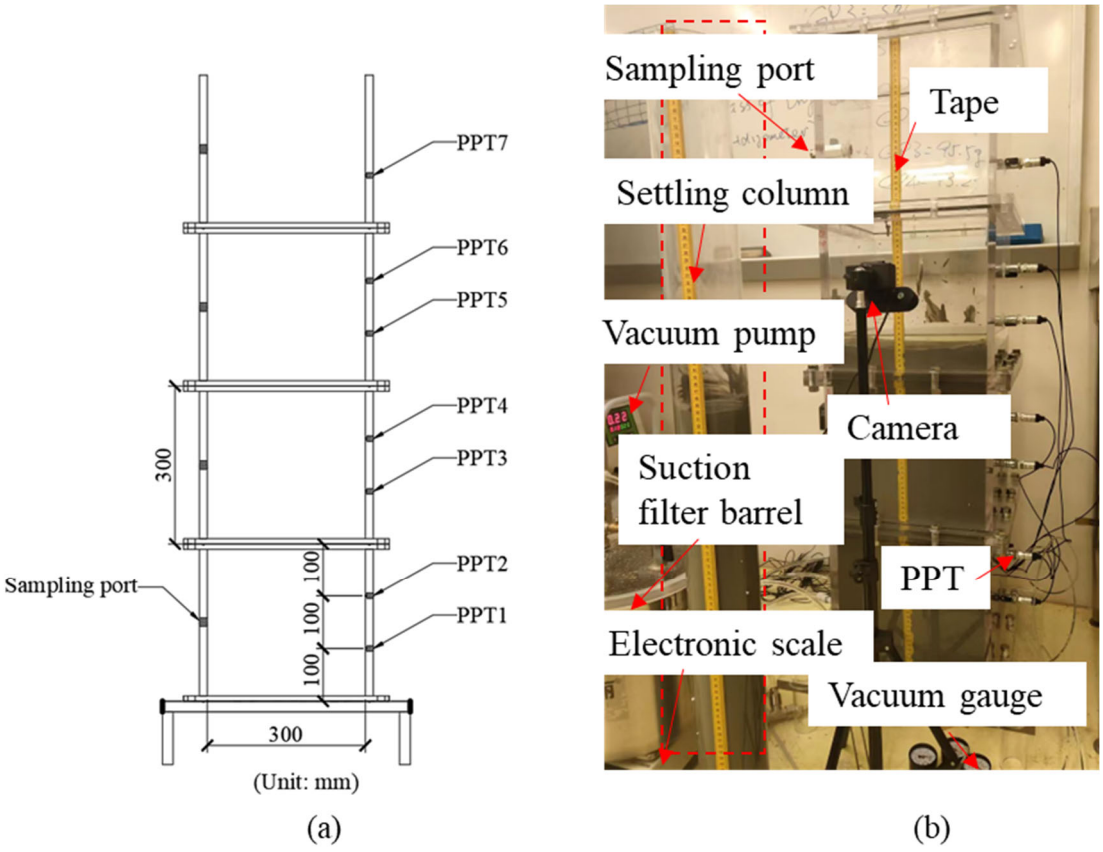

Figure 2–Setup of model test applying PHD with vacuum preloading (a) scheme diagram of model box; (b) apparatus of model test

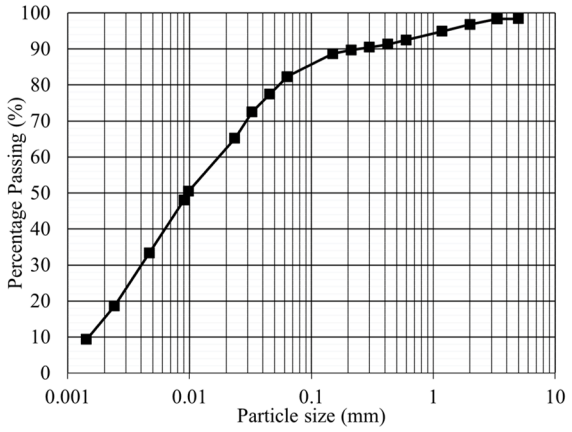

Figure 3–Particle size distribution curve of HKMD

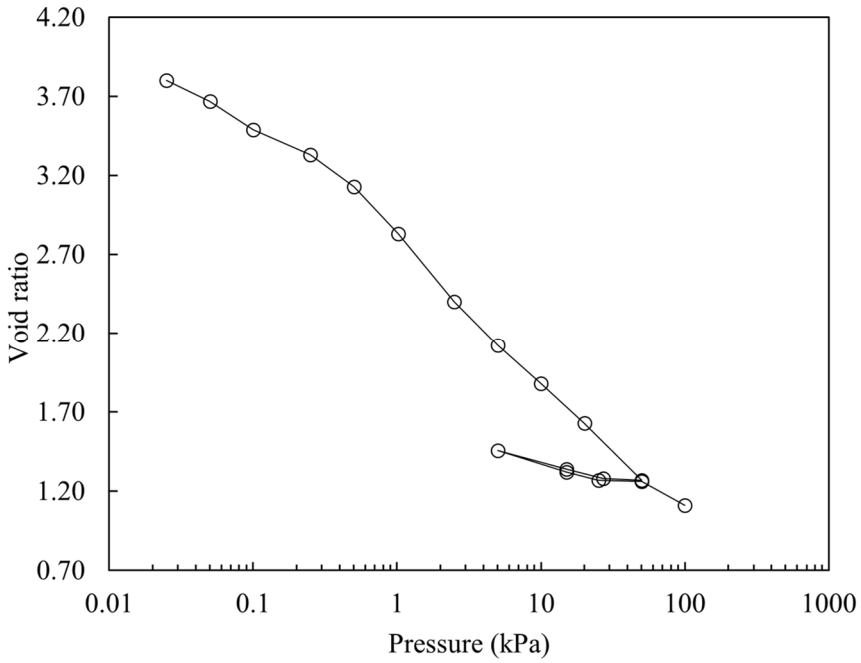

Figure 4–*e*-log *σz'* curves of HKMD

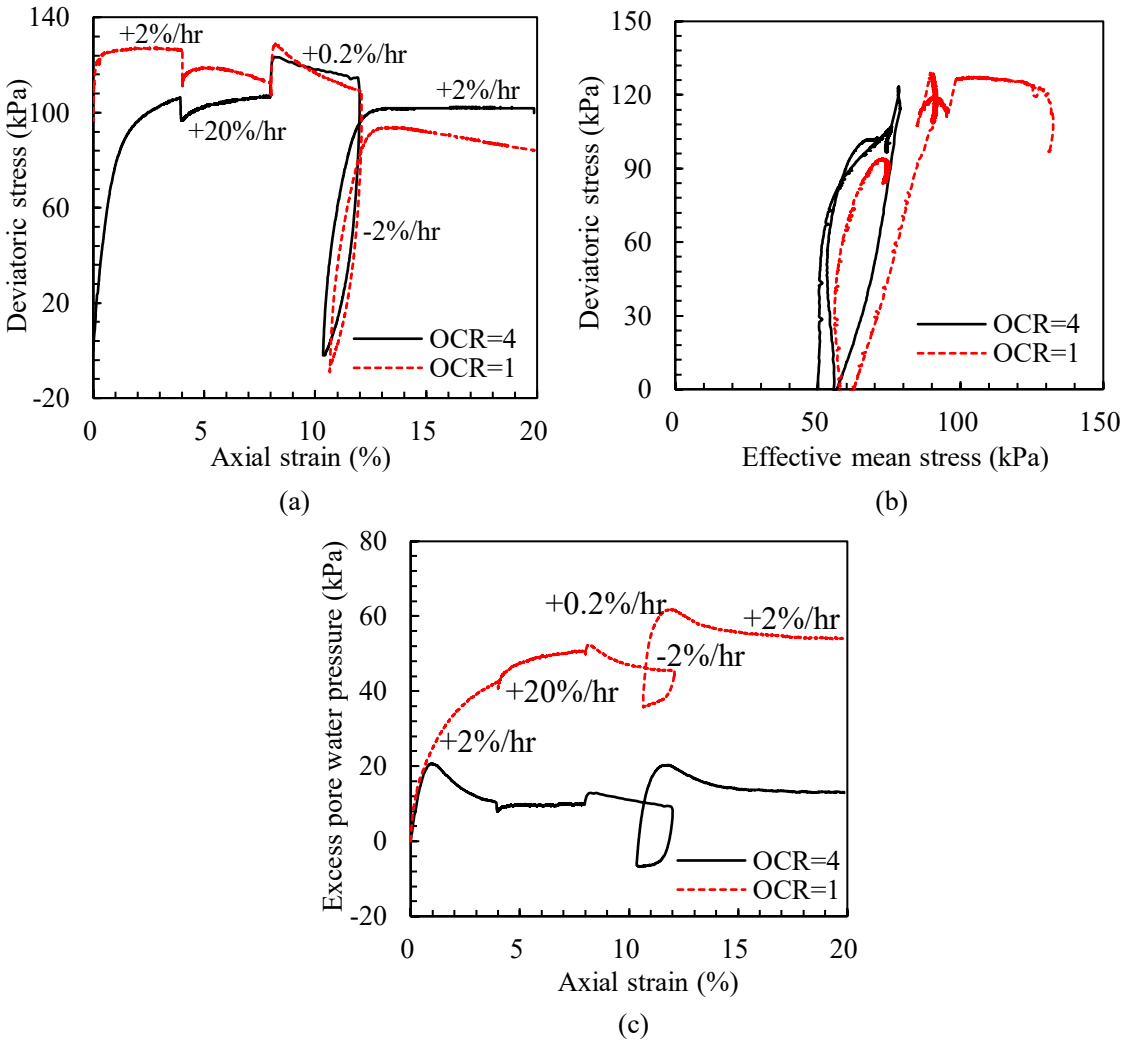

Figure 5–Triaxial test results of the HKMD: (a) deviatoric stress versus axial strain; (b) deviatoric stress versus effective mean stress; (c) excess pore water pressure axial strain

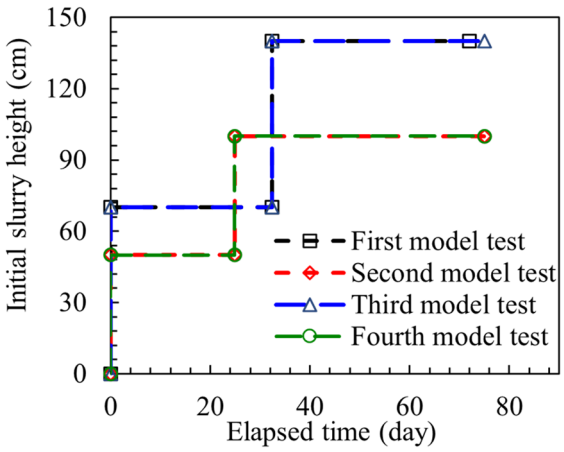

Figure 6–Initial slurry height with time of four model tests

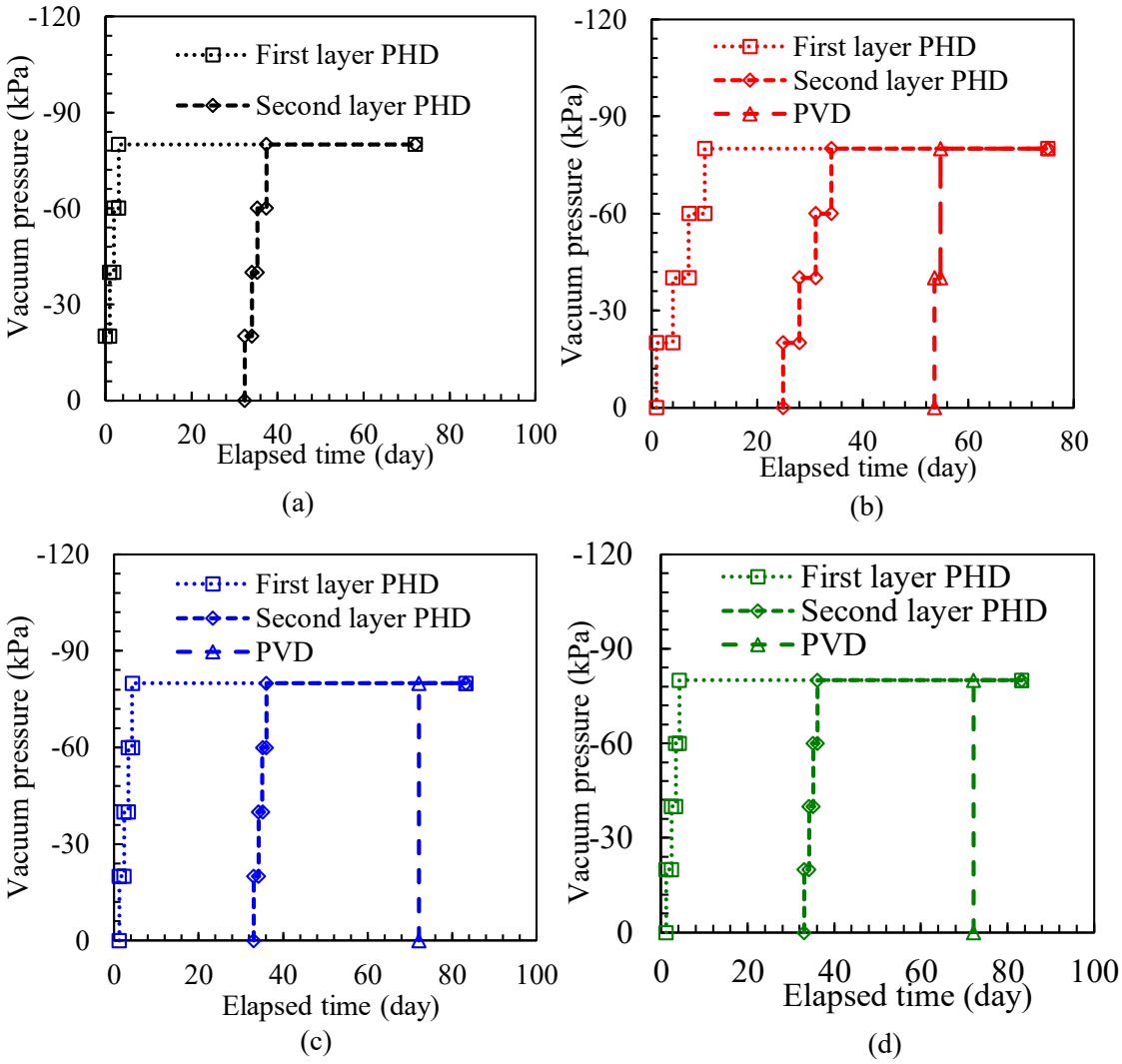

Figure 7–Vacuum consolidation scheme of four model tests: (a) the first model test; (b) the second model test; (c) the third model test; (d) the fourth model test

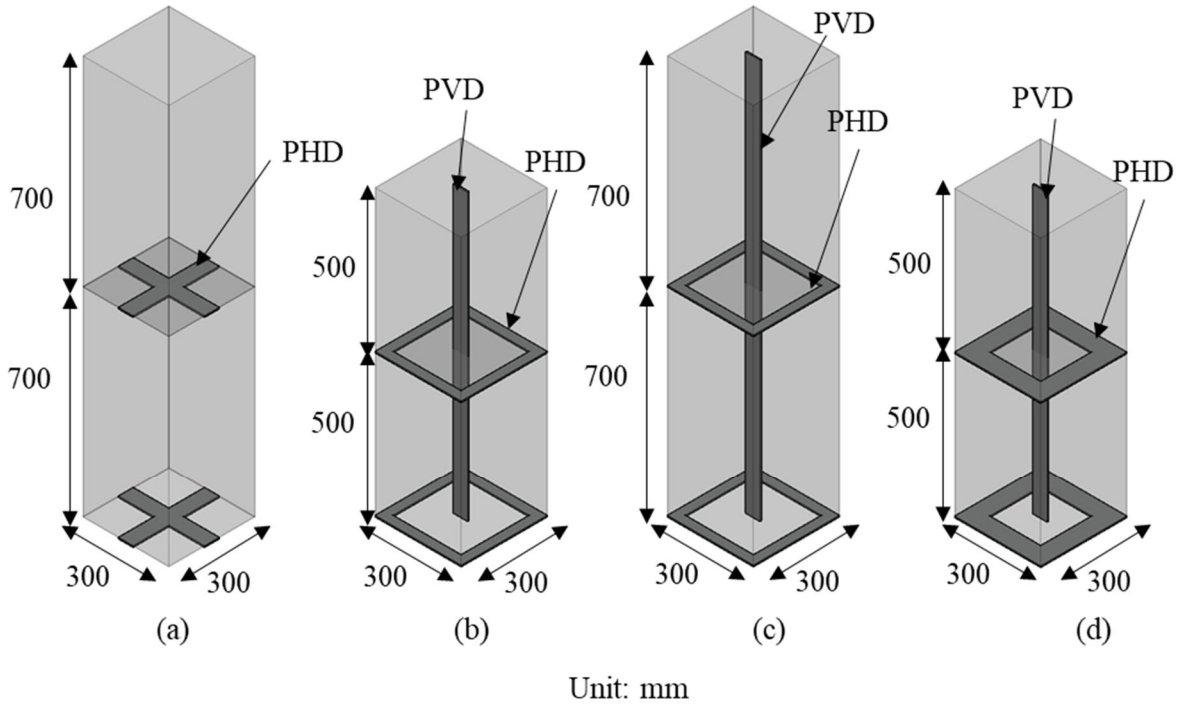

Figure 8–Sketch of four model tests: (a) first model test; (b) second model test; (c) third model test; (d) fourth model test

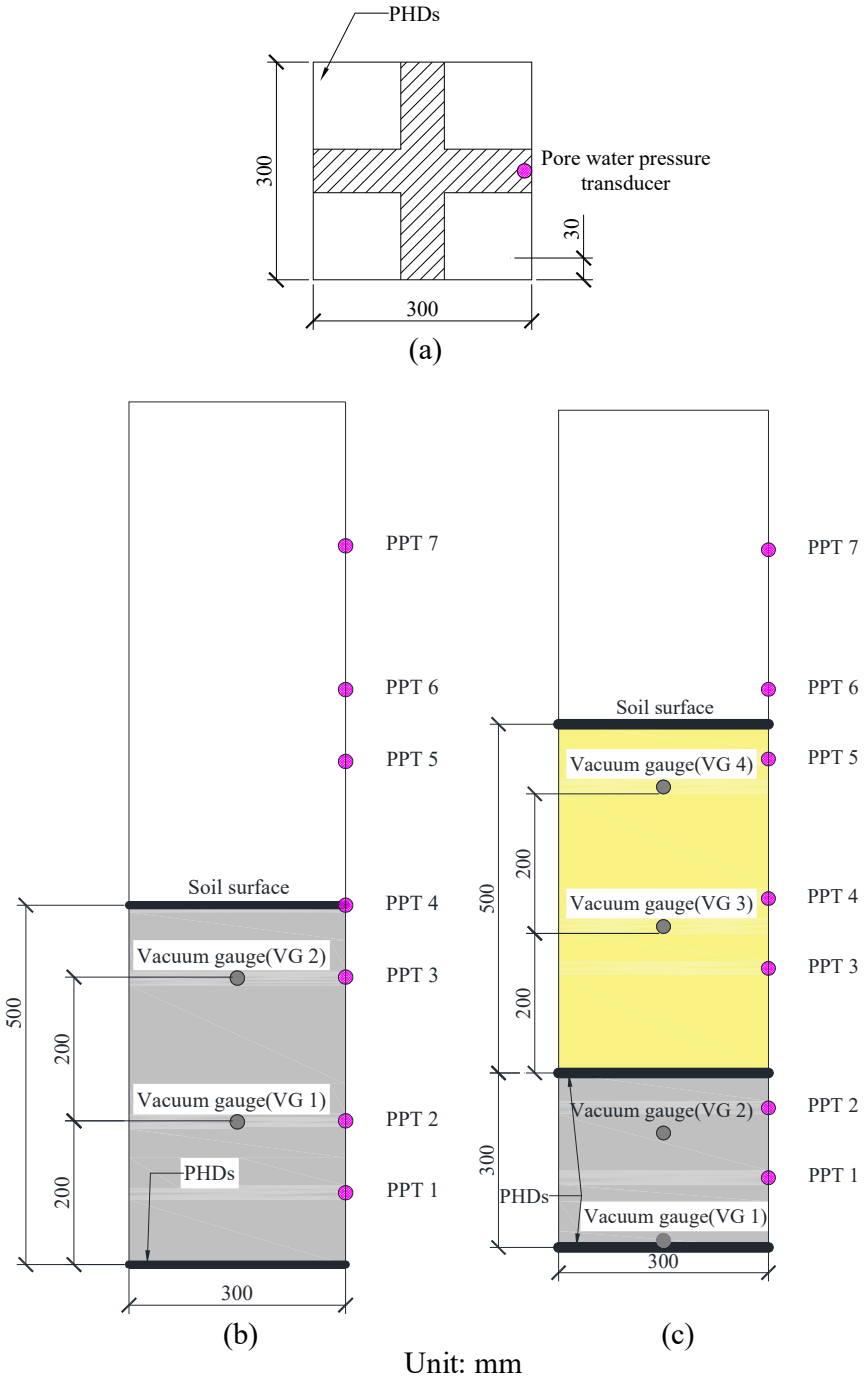

Figure 9–Instrumentation of the second model test: (a) top view; (b) front view of the first layer PHDs vacuum preloading; (c) front view of the second layer PHDs vacuum preloading

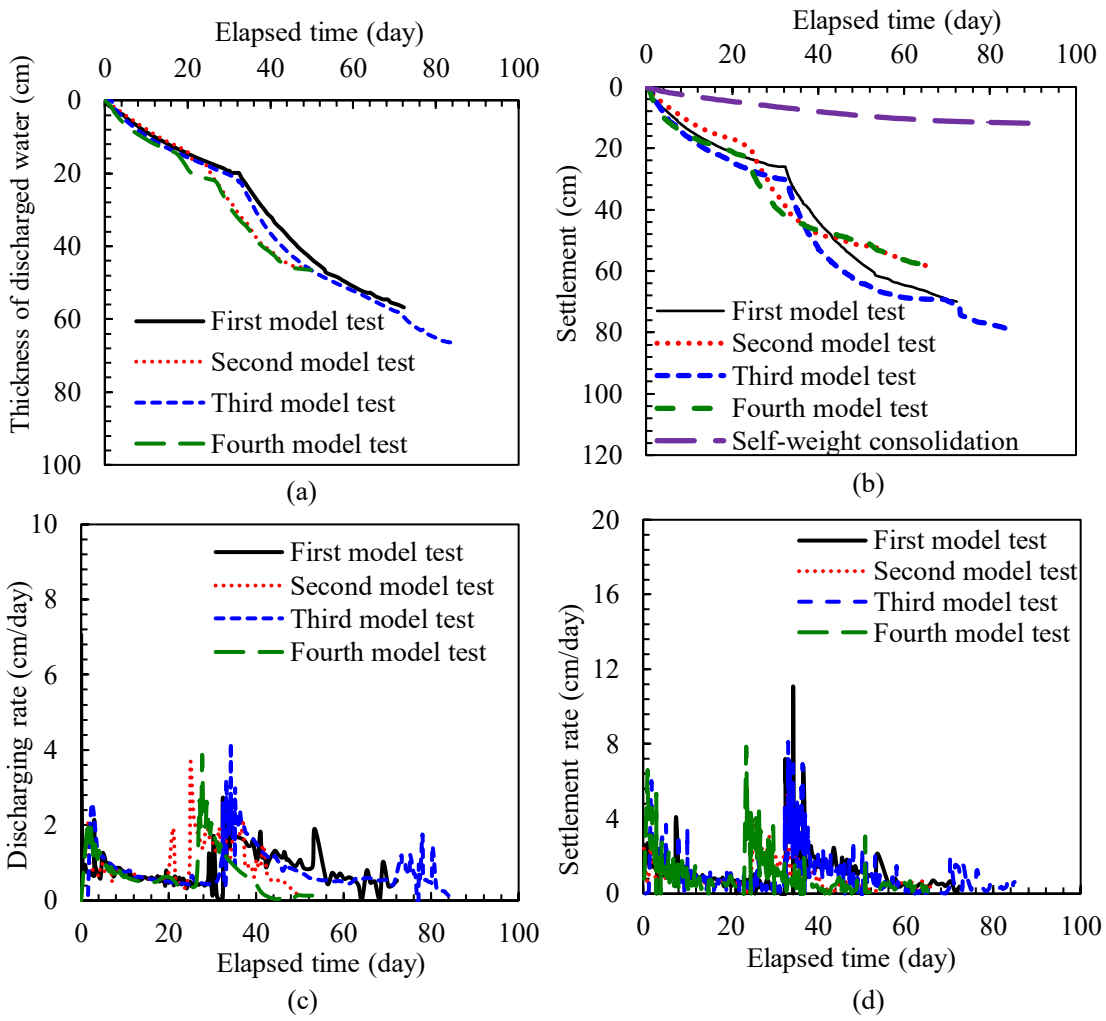

Figure 10–Discharged water with time of four physical model tests: (a) thickness of discharged water; (b) settlement; (c) discharging rate; (d) settlement rate

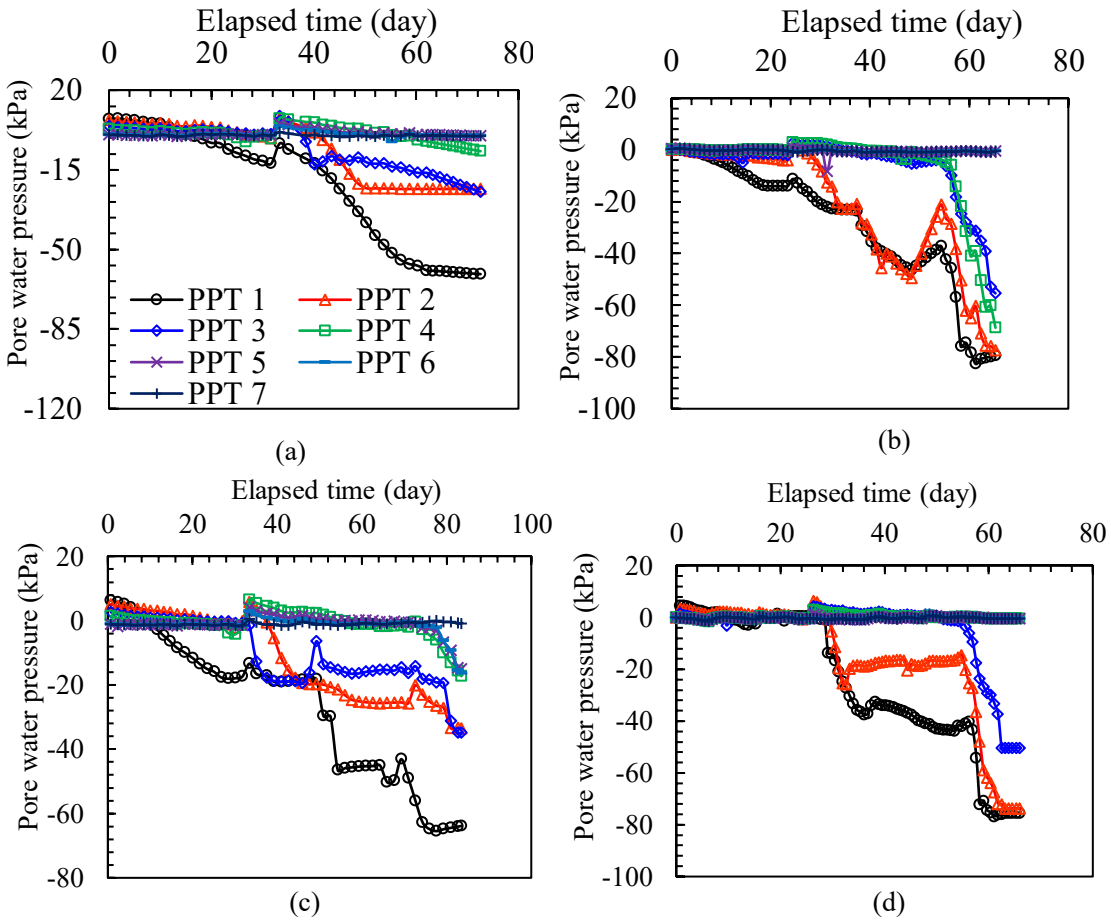

Figure 11–Pore water pressure with time of four physical model tests: (a) first model test; (b) second model test; (c) third model test; (d) fourth model test

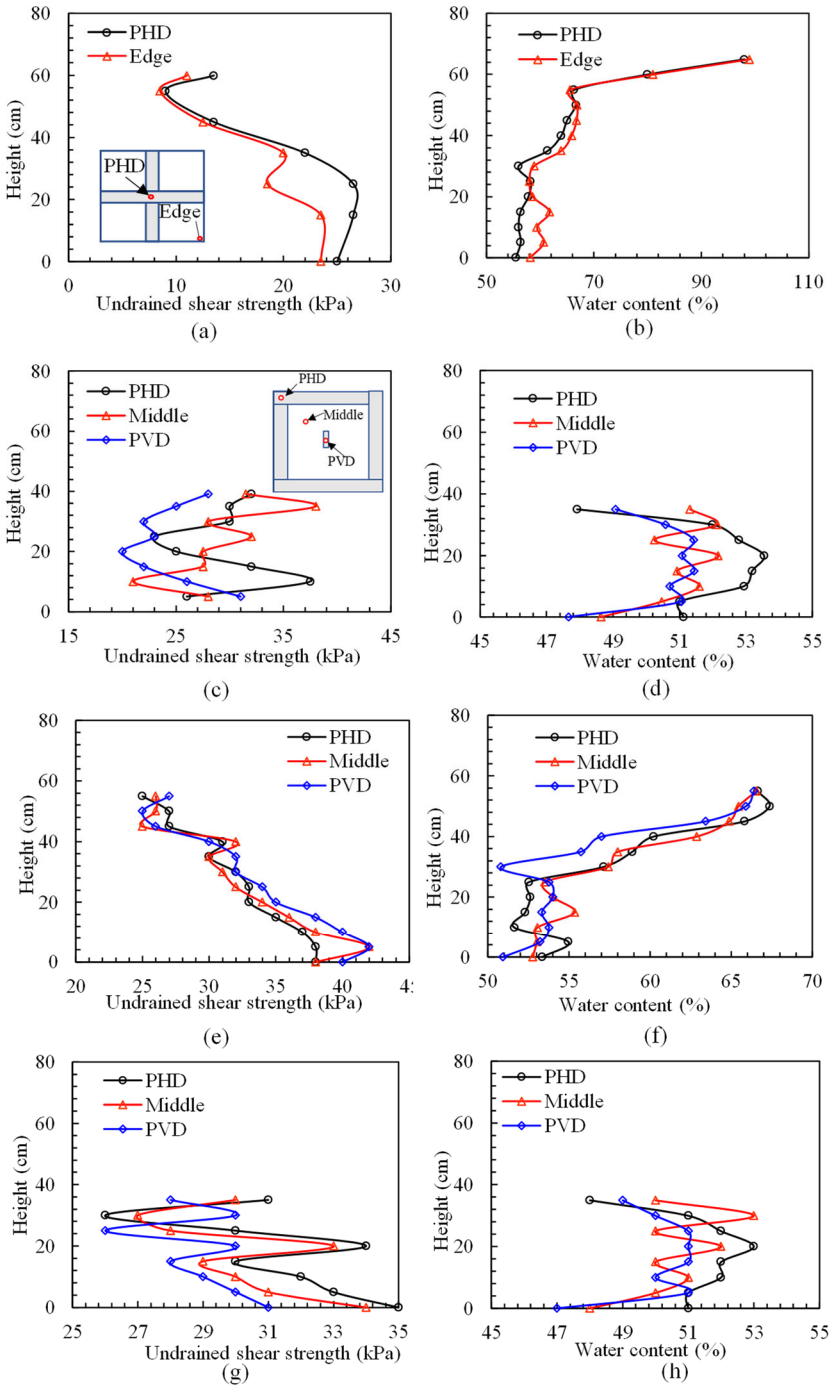

Figure 12–Undrained shear strength and water content profile at the end of different model tests: (a) undrained shear strength (first model test); (b) water content profile(first model test); (c) undrained shear strength (second model test); (d) water content profile (second model test); (e) undrained shear strength profile (third model test); (f) water content profile (third model test); (g) undrained shear strength profile (fourth model test); (h) water content profile (fourth model test)

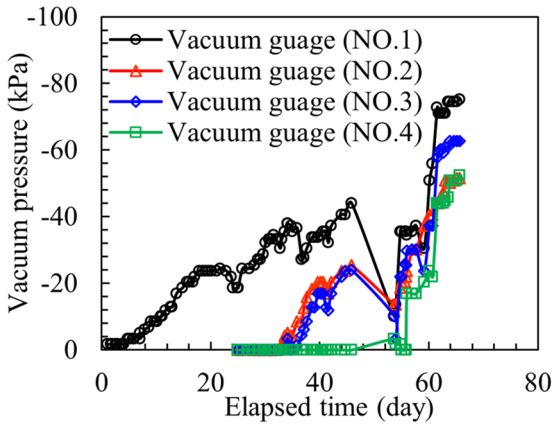

Figure 13–Vacuum pressure distribution of the second model test

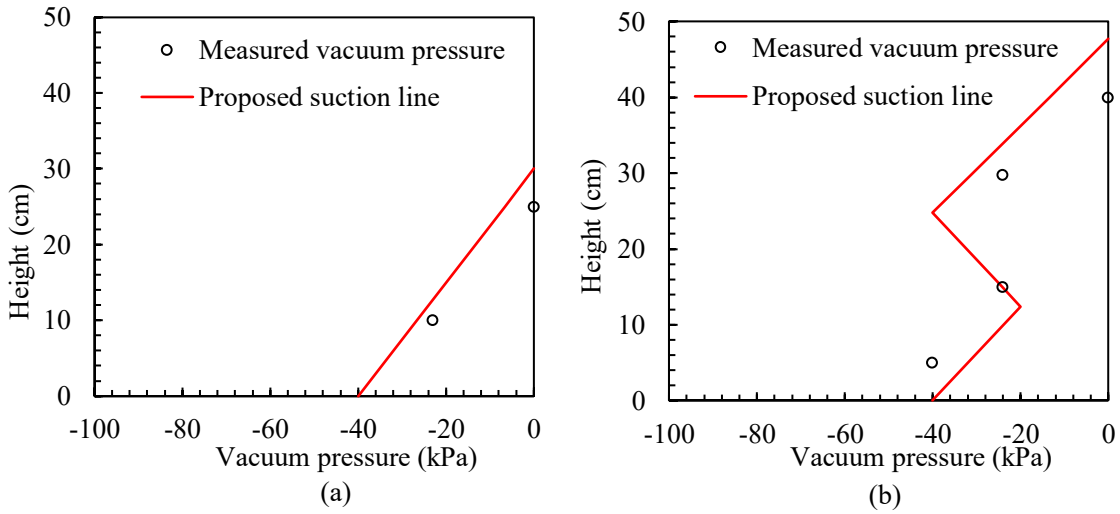

Figure 14–Vacuum pressure distribution profile: (a) PHDs vacuum preloading for one layer of soil; (b)

PHDs vacuum preloading PHDs vacuum preloading for two layers of soil

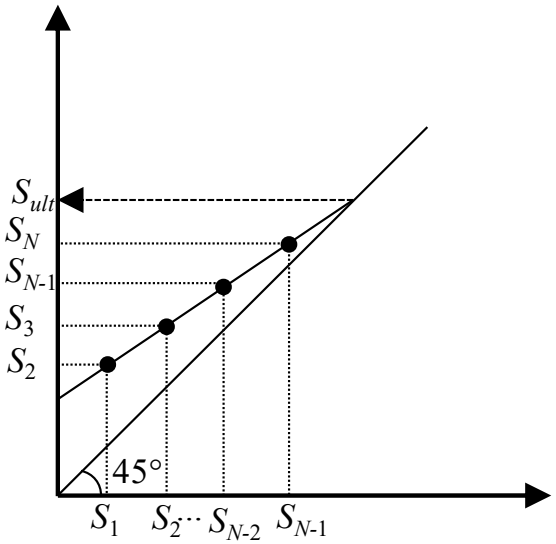

Figure 15–Schematic illustration of Asaoka's method

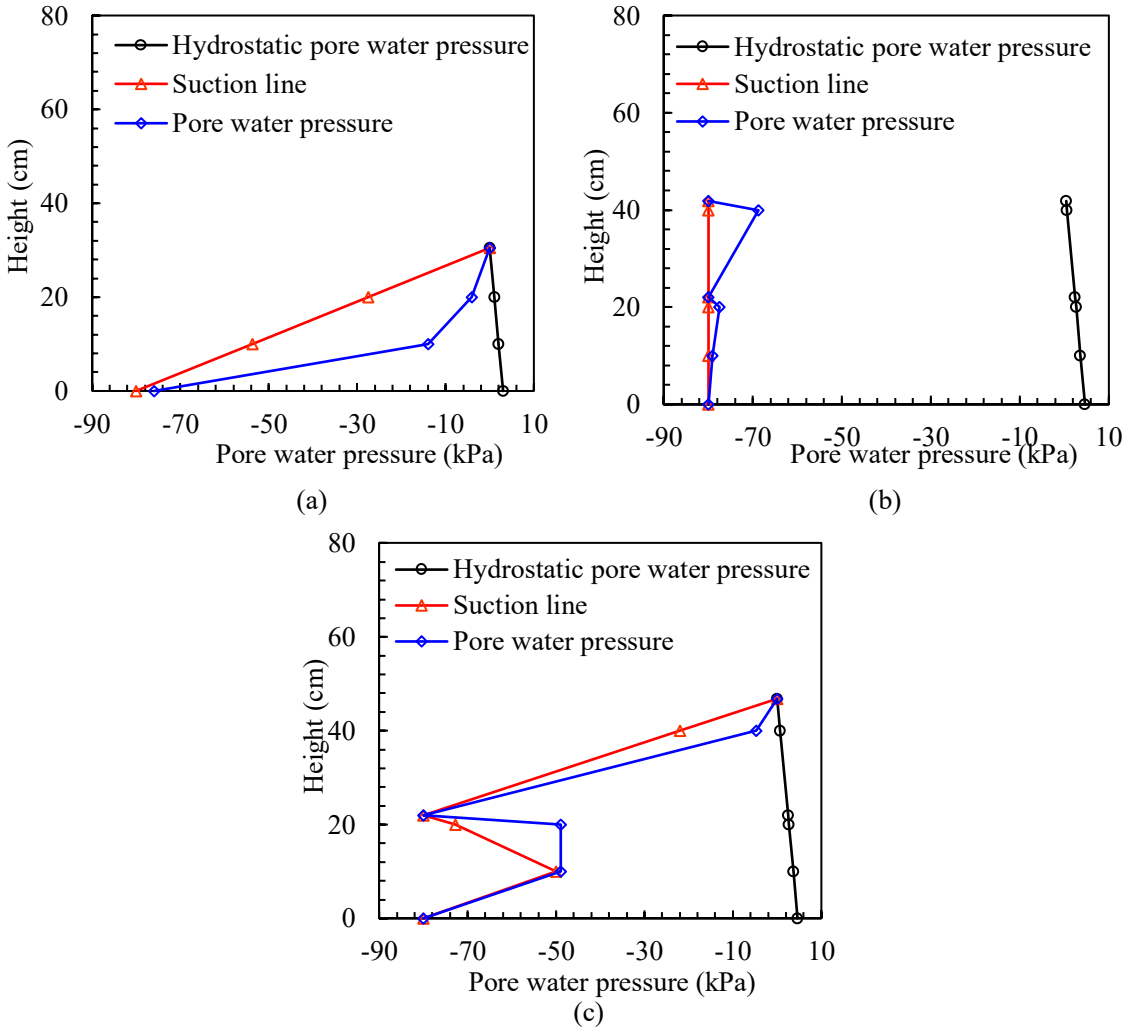

Figure 16–Pore water pressure distribution profile of the second model test: (a) after one layer PHDs vacuum preloading; (b) after two layer PHDs vacuum preloading; (c) after two layer PHDs vacuum preloading and PVD vacuum preloading

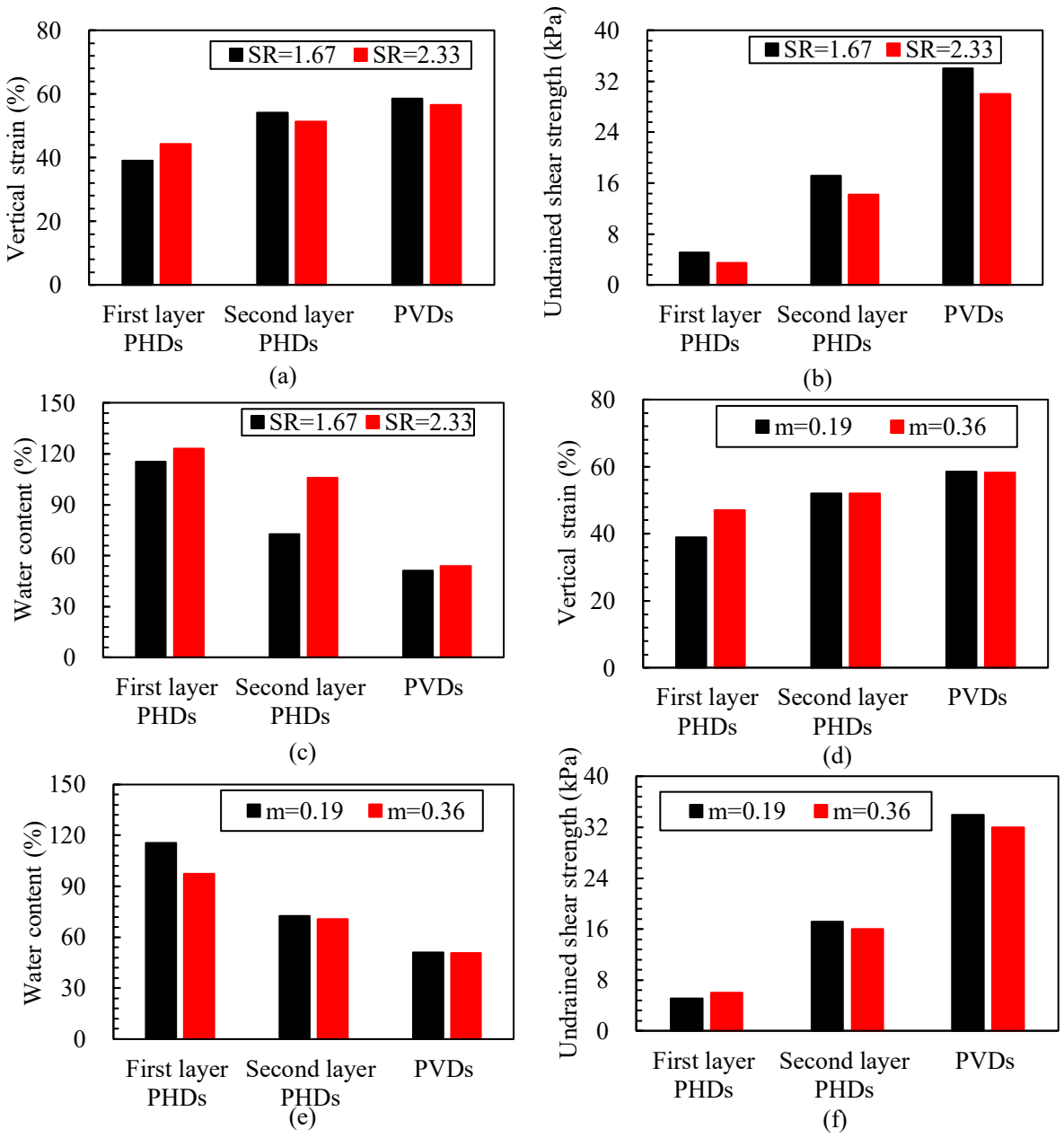

Figure 17–Parametric studies: (a) vertical strain of different SR; (b) water content of different SR; (c) undrained shear strength of different SR; (d) vertical strain of different *m*; (e) water content of different *m*; (f) undrained shear strength of different *m*